



Deposition of Pd nanoparticles on TiO₂ using a Pd(acac)₂ precursor for photocatalytic oxidation of CO under UV-LED irradiation



D.S. Selishchev^{a,b,*}, N.S. Kolobov^a, A.V. Bukhtiyarov^a, E.Y. Gerasimov^a, A.I. Gubanov^{b,c}, D.V. Kozlov^{a,b}

^a Boreskov Institute of Catalysis, Novosibirsk 630090, Russian Federation

^b Novosibirsk State University, Novosibirsk 630090, Russian Federation

^c Nikolaev Institute of Inorganic Chemistry, Novosibirsk 630090, Russian Federation

ARTICLE INFO

Keywords:

Photocatalytic oxidation
CO oxidation
TiO₂
Pd nanoparticles
Pd(acac)₂

ABSTRACT

In this study, 0.1–4 wt.% Pd-loaded catalysts were synthesized via thermal decomposition of palladium (II) acetylacetone (Pd(acac)₂) at 210–310 °C or its photodecomposition under UV-LED irradiation using anatase TiO₂ as a support. The catalysts were characterized by X-ray fluorescence, AAS, TEM, XPS, and CO chemisorption analyses and tested for CO oxidation at room temperature in a batch reactor both in the absence and presence of UV-LED irradiation. The effects of the Pd(acac)₂ decomposition method and Pd content on the dark catalytic and photocatalytic activities were studied.

Decomposition of Pd(acac)₂ occurred with the formation of the metallic (Pd⁰) and oxidized (PdO) forms of palladium on the TiO₂ surface for both employed methods. The photodecomposition resulted in an increased amount of metallic palladium. All of the synthesized Pd/TiO₂ catalysts completely oxidized CO to CO₂ at room temperature. UV-LED irradiation with a total irradiance of 10.4 mW/cm² in the UVA region increased the rate of CO oxidation by up to 5 times compared to dark catalytic oxidation. Photodecomposition of Pd(acac)₂ resulted in a higher activity of the Pd/TiO₂ catalysts compared to the thermal decomposition method. The rate of CO oxidation under UV irradiation and under dark conditions monotonically increased as the Pd content increased due to the stability of high dispersion of Pd particles even with a high Pd content. The maximum value of the photonic efficiency was estimated to be 5.9%.

CeO₂, SiO₂, and Al₂O₃ were also employed for the deposition of Pd to investigate the effect of a semiconducting support. For the CeO₂-based catalyst, the activity under UV irradiation was higher than in the dark, but this effect was much lower compared to that of catalysts based on TiO₂. By contrast, no substantial difference in the CO oxidation rate in the absence and presence of UV irradiation was observed for the non-semiconducting supports, SiO₂ and Al₂O₃, confirming the photocatalytic oxidation of carbon monoxide for the TiO₂- and CeO₂-based catalysts.

1. Introduction

An important task facing humankind at present is the control of environmental pollution. A high level of the emissions from industry and motor transport has a pernicious influence on the quality of air and water in the cities. According to the World Health Organization's report in 2012, ca. 6.5 million people die every year due to the diseases associated with exposure to polluted air indoors and outdoors [1].

Advanced oxidation processes (AOPs) have shown great promise as a more energy efficient and sustainable alternative to conventional processes, including adsorption, non-catalytic and catalytic combustion, chlorination, etc., for the removal and decomposition of air and

water pollutants. AOPs include electrolysis, Fenton and photo-Fenton systems, O₃/H₂O₂ and O₃/UV systems, photocatalysis, etc. Despite the different system compositions, all of systems are based on the generation of high-power oxidants, such as hydroxyl (OH[•]) or sulfate (SO₄²⁻) radicals [2]. Hydroxyl radical-based AOPs were first proposed in the 1980s for the purification of water [3]. Later, this concept was extended to processes with sulfate radicals [4–6].

The most commonly used process among AOPs for air purification is the heterogeneous photocatalytic oxidation (PCO) resulting in the decomposition of air pollutants on the surface of a UV- or visible light-irradiated photocatalyst under ambient temperature and humidity. Titanium dioxide attracts great attention as a photocatalyst in this field

* Corresponding author at: Boreskov Institute of Catalysis, Novosibirsk 630090, Russian Federation.
E-mail address: selishev@catalysis.ru (D.S. Selishchev).

due to its low cost, chemical stability, and commonly, complete mineralization of pollutants to harmless products under UVA irradiation at a high rate [7–10]. PCO of many volatile organic compounds (VOCs), including alcohols, aldehydes, ketones, hydrocarbons, N-, P-, F-, Cl-, and S-containing compounds, over TiO_2 -based photocatalysts has been described [11–17]. In addition to VOCs, some inorganic pollutants, such as NH_3 , NO_x , H_2S , and SO_x , can also be oxidized on the TiO_2 surface [17–21].

One more harmful inorganic air pollutant is carbon monoxide. CO is a major concern for safe living environments because it exists as the largest single component in emissions among all pollutants [22]. In addition, our previous studies have shown that CO is a by-product of the PCO of many organic compounds [23,24].

Thermal oxidation of carbon monoxide over TiO_2 modified with noble metals (e.g., Au, Pt, etc.) is a well-studied process [25–29]. These M/ TiO_2 systems have also been employed for the photocatalytic oxidation of CO under ambient conditions when, instead of becoming thermal energy, the light energy absorbed by the photocatalyst applied toward the acceleration of the reaction at room temperature [30]. The photocatalytic oxidation of CO on the pure TiO_2 surface under UV irradiation was shown to be a very slow process, and the deposition of Pt particles on the TiO_2 surface substantially increased the reaction rate [31,32]. Karakas and Yetisemiyen [33] investigated the Pd/ TiO_2 and Pd/ TiO_2 - SiO_2 catalysts for PCO of carbon monoxide at room temperature under UV irradiation, and they reported that Pd/ TiO_2 exhibits a higher photocatalytic activity. The TiO_2 catalyst supported with Pd-Pt bimetallic nanoparticles with an enhanced photocatalytic activity in CO oxidation in the presence of humidity was described [30,34].

Studies of CO PCO under visible light were also published, but they received much less attention [35,36]. Deng et al. [37] employed oxygen and argon plasmas to activate the Au/ TiO_2 photocatalyst for CO oxidation under visible light. The authors demonstrated that activation by oxygen plasma substantially enhances the photoactivity of Au/ TiO_2 under visible light.

The reaction mechanism of the CO photocatalytic oxidation over the M/ TiO_2 catalysts was proposed to involve the transfer of photo-generated electrons from TiO_2 to the metal particle, reducing their energy due to different values of the work function in the conduction band of TiO_2 and in the metal [38]. Further, the interfacial transfer of electrons from the metal to oxygen adsorbed on the metal surface occurs and results in the formation of surface active forms of oxygen, such as O_2^{2-} and $\text{O}^{\bullet-}$, which oxidize adsorbed CO molecules [25,39].

The charge state of the metal and the size of their particles on the TiO_2 surface play an important role. Many studies have shown that the noble metal in the metallic form leads to higher photocatalytic activity than the oxidized forms. Vorontsov et al. [40] investigated the effect on the quantum efficiency of various forms of Pt photodeposited on the TiO_2 surface in PCO of acetone vapor and CO. For both substrates, the photocatalytic activity increased as the charge state of Pt decreased. An optimal size of the metal particles, providing the fastest interface transfer of electrons, also exists [41].

Therefore, the method for metal deposition is a key factor for producing a highly active photocatalyst. Kozlova et al. [42] deposited Pt on TiO_2 via the chemical reduction or photoreduction of H_2PtCl_6 . The chemical reduction method resulted mainly in the metallic form of Pt, and the photodeposition led to a high amount of Pt in oxidized forms. Additionally, we previously studied CO PCO over Pt-, Pd-, and Au-loaded photocatalysts prepared via the chemical reduction or photoreduction of chlorinated inorganic precursors. In the case of platinum, the chemical reduction method resulted in a much higher activity of Pt/ TiO_2 compared to the photodeposition [43].

Cl atoms from chlorinated inorganic precursors may poison the photocatalyst surface and reduce its activity. At the same time, Wang et al. [44] synthesized the Pd-loaded catalysts from various precursors, including PdCl_2 , $[\text{Pd}(\text{NH}_3)_4](\text{NO}_3)_2$, or Pd(acac)₂, and reported that Pd(acac)₂ resulted in the best dispersion of palladium nanoparticles and

the highest activity of Pd/ TiO_2 in dark CO oxidation (i.e., without UV irradiation) at room temperature. In addition, the deposition of Pd nanoparticles in the metal form only with a narrow size distribution was achieved on the SiO_2 support by low-temperature (~ 200 °C) decomposition of Pd(acac)₂ [45].

Therefore, the usage of metal-organic precursors may be preferable for the deposition of highly dispersed metal nanoparticles on the TiO_2 surface, producing a highly active photocatalyst. In a previously published paper [46], we showed that the thermal decomposition of Pd(acac)₂ is a good method for the synthesis of Pd/ TiO_2 with a high photocatalytic activity in CO oxidation under UV irradiation. Two advantages were achieved using a Pd(acac)₂ precursor. First, Pd(acac)₂ does not contain chlorine atoms, which could otherwise remain on the photocatalyst surface and decrease the quantum efficiency of the process, acting as the sites for the recombination of photogenerated charge carriers. Second, Pd(acac)₂ decomposes at a low temperature (~ 200 °C) resulted in no decreasing in the specific surface area of the photocatalyst. This study continues that work and aims to investigate another preparation method of Pd/ TiO_2 photocatalysts via the photodeposition and to compare with the thermal deposition.

The photodeposition method is based on the reduction of metal ions by photogenerated electrons formed under UV irradiation of TiO_2 , while photogenerated holes interact with electron donors. Typically, the preparation technique includes slurring photocatalyst in water with addition of an electron donor (e.g., ethanol) and irradiation of slurry for an extended period under continuous stirring [47,48]. Here, we present new data on the direct photodecomposition of Pd(acac)₂ on the TiO_2 surface under long-term UV irradiation resulted in the formation of Pd nanoparticles. This method has an advantage compared to the conventional photodeposition technique because Pd(acac)₂ contains itself electron donor (i.e., organic ligand) that simplifies the preparation or allows for the formation of Pd nanoparticles directly during the photocatalytic process. Additionally, the stability of a high dispersion of Pd particles may be achieved even at a high Pd content.

In this study, the effects of the Pd(acac)₂ decomposition method and Pd content as well as the type of support on CO oxidation under ambient conditions both in the absence and presence of UV irradiation are described. The photonic efficiency of this process is estimated, and a comparison with the Pt/ TiO_2 photocatalyst prepared via the chemical reduction of H_2PtCl_6 is given.

2. Experimental

2.1. Materials

The following powdered materials were employed as supports for palladium deposition: TiO_2 Hombifine N (100% anatase, $a_s(\text{BET}) \sim 350$ m^2/g) purchased from Sachtleben Chemie GmbH (Germany), CeO_2 (fluorite-type, $a_s(\text{BET}) \sim 50$ m^2/g) and SiO_2 (X-ray amorphous, $a_s(\text{BET}) \sim 440$ m^2/g) purchased from Sigma-Aldrich (USA), and Al_2O_3 (γ -phase, $a_s(\text{BET}) \sim 180$ m^2/g) purchased from AO AZKIOS (Russia). All the supports were washed thoroughly with deionized water and dried at 120 °C.

Palladium (II) acetylacetone (Pd(acac)₂) powder synthesized in a laboratory was used as a Pd precursor. The synthesis of Pd(acac)₂ was performed as follows [49]: 0.50 g of $\text{Pd}(\text{NO}_3)_2 \times 2\text{H}_2\text{O}$ purchased from Aurat JSC (Russia) was dissolved in 10 mL of acetone (CH_3COCH_3). Then, 0.40 g of acetylacetone ($\text{CH}_3\text{COCH}_2\text{COCH}_3$) was added. The acetone and acetylacetone used during synthesis were high purity grade and were applied as purchased from AO REAHIM (Russia) without further purification. Then, the reaction mixture was stirred for 5 min. The formed Pd(acac)₂ crystals were filtered, washed with acetone and dried in the air. The Pd content was measured by X-ray fluorescence analysis (XRF) using an ARL ADVANT'X spectrometer (Thermo Fisher Scientific, USA) with a rhodium anode. Table 1 shows the measured Pd content in the synthesized Pd(acac)₂, which is similar to the theoretical

Table 1
Theoretical and experimental Pd content.

Sample	Theoretical Pd content, wt. %	Experimental Pd content, wt. %	
		XRF	AAS
Pd(acac) ₂	34.93	34.88	
Pd(acac) ₂ /TiO ₂	0.1	0.09	0.06
	0.5	0.48	0.42
	1.0	0.98	0.94
	2.0	1.87	
	4.0	4.33	
Pd(acac) ₂ /CeO ₂	2.0	2.14	
Pd(acac) ₂ /SiO ₂	2.0	2.03	
Pd(acac) ₂ /Al ₂ O ₃	2.0	1.87	

value. The crystal phase of Pd(acac)₂ was determined by XRD analysis. The XRD pattern for synthesized Pd(acac)₂ can be found in Fig. S1 in the SI section.

2.2. Photocatalyst preparation

The Pd-loaded catalysts were synthesized via impregnation of the support with a certain amount of Pd(acac)₂ dissolved in acetone followed by the evaporation of acetone and the decomposition of Pd(acac)₂ during thermal or UV treatment.

Typically, 5 g of a support was suspended in 40 mL of acetone and stirred at 500 rpm for 30 min. A certain amount of Pd(acac)₂ was added to 5 mL of acetone and heated to 40 °C to allow for its complete dissolution. The Pd content in the photocatalysts was varied from 0.1 to 4 wt.% (Table 1). The Pd(acac)₂ solution was added dropwise to the suspension of the support. The suspension was adjusted at 40 °C under continuous stirring at 500 rpm until the evaporation of acetone. Finally, acetone was completely evaporated using a vacuum pump. The deposition of Pd(acac)₂ resulted in a change in color of TiO₂ as well as SiO₂ and Al₂O₃ from white to light brown. Typical UV-vis diffuse reflectance spectra for TiO₂ supported with Pd(acac)₂ can be found in Fig. S3 in the SI section. The obtained samples with deposited Pd(acac)₂ are referred to as wPd(acac)₂/S, where w is the theoretical Pd content, S is TiO₂, CeO₂, SiO₂, or Al₂O₃. The Pd content in the wPd(acac)₂/S samples was measured using XRF analysis, as described above. Additionally, atomic absorption spectroscopy (AAS) using an iCE 3000 spectrometer (Thermo Fisher Scientific, USA) was employed for analysis of the catalysts with Pd content less than 1 wt.% because XRF method has a low accuracy in this content range. The data for both methods agreed with each other. The results for all the synthesized catalysts are shown in Table 1. The measured contents were close to the theoretically calculated values.

The following methods were employed for the further treatment of the wPd(acac)₂/S samples to completely decompose Pd(acac)₂:

1) Thermal decomposition:

The thermal decomposition method is based on the thermal treatment of the sample at a temperature higher than the decomposition temperature of Pd(acac)₂. According to the thermogravimetric analysis using an STA 449 C instrument from Netzsch (Germany), Pd(acac)₂ starts to decompose ca. 185 °C (Fig. S2 in the SI section). Therefore, the temperatures of 210, 250 or 310 °C were selected for the calcination of the samples. Typically, 1 g of the wPd(acac)₂/S sample was calcined at 210, 250 or 310 ± 5 °C in the air for 3 h. The TiO₂-based catalysts prepared by this method are referred to as wPd/TiO₂-T, where w is the theoretical Pd content from Table 1, and T is 210, 250 or 310 according to the calcination temperature. For the CeO₂, SiO₂, and Al₂O₃ supports, the theoretical Pd content was only 2 wt.% (Table 1) and the calcination temperature was only 210 °C. These samples are referred to as 2Pd/CeO₂-210, 2Pd/SiO₂-210, and 2Pd/Al₂O₃-210, respectively.

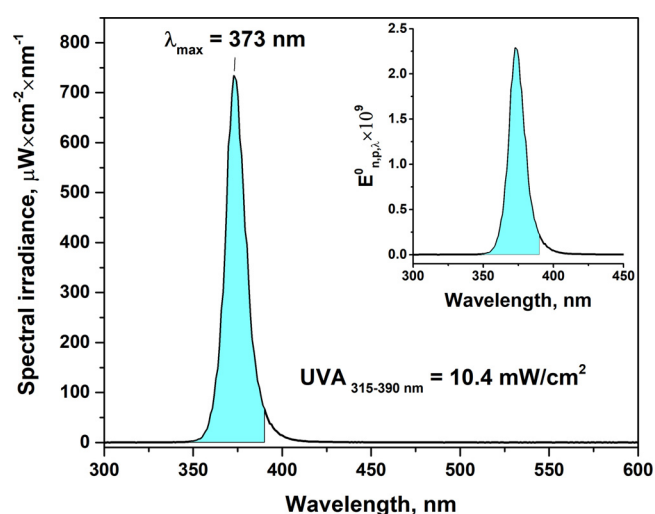


Fig. 1. Emission spectrum of the UV-LED used for catalyst irradiation. The inset shows the spectral photon irradiance $E_{n,\lambda,0}^0 \times 10^9$.

2) Photodecomposition:

The photodecomposition method was employed for the TiO₂-based sample only because this support can decompose the Pd(acac)₂ precursor by forming photogenerated charge carriers (i.e., electrons and holes) under UV irradiation. CeO₂ was not employed for this method due to its low photocatalytic activity. Typically, 9 mg of the wPd(acac)₂/TiO₂ sample was uniformly deposited on a 9.1 cm² glass plate and irradiated overnight using a high-power UV light-emitting diode (UV-LED) from Nichia Corporation (Japan). The total irradiance in the region of 315–390 nm was 10.4 mW/cm² (Fig. 1). The formation of CO₂ was detected during the UV irradiation of wPd(acac)₂/TiO₂ samples, which confirms the decomposition of Pd(acac)₂ on the UV-irradiated TiO₂ surface with the oxidation of organic ligands to carbon dioxide. The typical kinetic plot for CO₂ accumulation during the irradiation of TiO₂ supported with Pd(acac)₂ is shown in Fig. 2. An intense CO₂ accumulation was observed after turning the UV-LED on. CO₂ concentration reached a constant value after long-term irradiation. CO₂ accumulation plot during the irradiation of TiO₂ alone also is shown in Fig. 2 for comparison. The CO₂ formation in the case of TiO₂ was due to the oxidation of organic impurities previously adsorbed on its surface and the photodesorption of CO₂. The TiO₂-based catalysts prepared

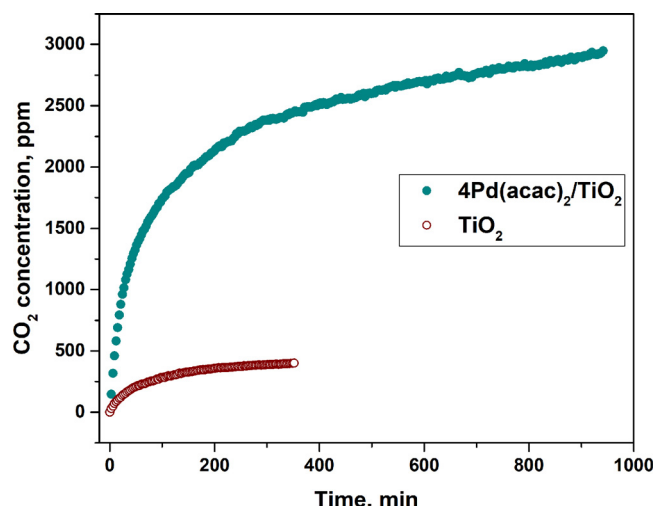


Fig. 2. Kinetic plots for CO₂ accumulation during the UV irradiation of 4Pd(acac)₂/TiO₂ and TiO₂ samples.

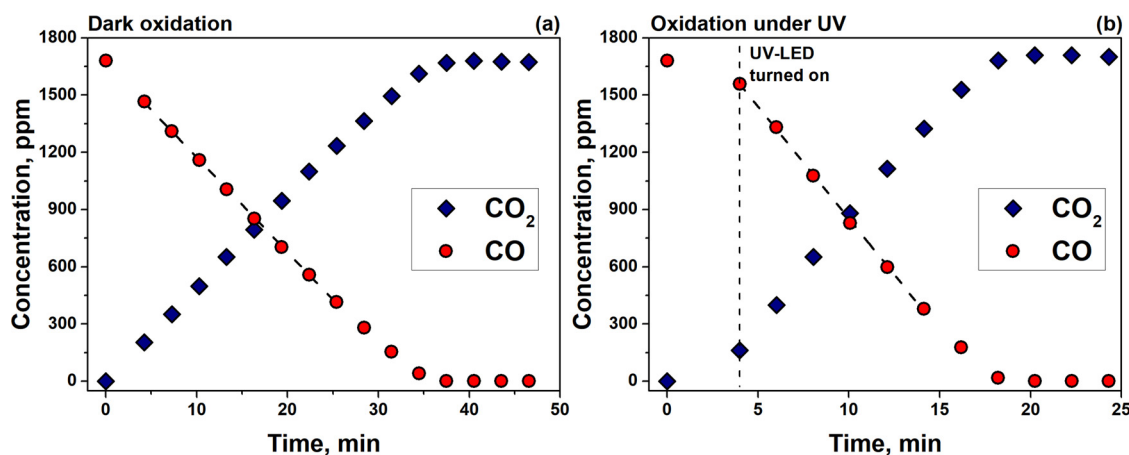


Fig. 3. Kinetic plots for CO removal and CO_2 accumulation during the CO oxidation over 4Pd/TiO₂-P in the dark (a) and under UV irradiation (b).

via this method are referred to as wPd/TiO₂-P, where w is the theoretical Pd content from Table 1, and P indicates the photo-decomposition method.

2.3. Characterization techniques

The morphology of the samples was investigated by TEM using a JEOL-2010 microscope (JEOL, Japan) at an accelerating voltage of 200 kV and a resolution of 0.14 nm. The microscope was equipped with an EDX spectrometer (XFlash, Bruker, Germany).

The surface composition of the synthesized catalysts was investigated using X-ray photoelectron spectroscopy (XPS). The photo-electron spectra were measured using a SPECS photoelectron spectrometer (SPECS Surface Nano Analysis GmbH, Germany) equipped with an AlK α ($\hbar\nu = 1486.6$ eV, 150 W) irradiation source. The binding energy (BE) scale was pre-calibrated using the positions of the Au4f_{7/2} (84.0 eV) and Cu2p_{3/2} (532.7 eV) photoelectron lines from metallic gold and copper foils. The background pressure at the analysis chamber did not exceed 8×10^{-7} Pa. Spectral analysis and data processing were performed with XPS Peak 4.1 software. The binding energy of the peaks was calibrated by the position of the Ti2p line at a BE of 458.8 eV from the TiO₂ support. For quantitative analysis, the integral intensities for the spectral regions of Ti2p, C1s, O1s, and Pd3d were corrected by their respective atomic sensitivity factors [50].

Chemisorption of CO was employed for the estimation of Pd dispersion. The measurements were performed using an AutoChem II 2920 chemisorption analyzer (Micromeritics, USA) in pulse mode with CO and He as the adsorbing and carrier gases, respectively [51]. Before the measurements, the catalysts were reduced under mild conditions. For this purpose, ca. 50 mg of sample was placed in a quartz tube and heated at 100 °C in a H₂ flow for 10 min. After cooling to 22 °C, the tube was blown with He, and 70- μL doses of CO at STP were injected under a pulse regime with 2 min intervals until complete saturation of the sample. The dispersion of Pd particles was estimated on the assumption of the stoichiometric adsorption of CO (i.e., CO/Pd_{surface} = 1) as follows:

$$D_{\text{Pd}} = \frac{N(\text{Pd}_{\text{surface}})}{N(\text{Pd}_{\text{total}})} = \frac{N(\text{CO})}{N(\text{Pd}_{\text{total}})}$$

where D_{Pd} is the dispersion of Pd particles, $N(\text{Pd}_{\text{surface}})$ is the number of surface Pd atoms, $N(\text{Pd}_{\text{total}})$ is the total number of Pd atoms, and $N(\text{CO})$ is the number of CO molecules adsorbed.

2.4. Kinetic experiments

The kinetic experiments for CO oxidation were performed in a 0.3 L batch reactor installed in the cell compartment of a Nicolet 380 FTIR

spectrometer (Thermo Fisher Scientific, USA). A schematic diagram and the details of the experimental setup have been described in our previous papers [24,52].

Typically, 91 mg of the sample was suspended in 10 mL of distilled water and treated using an ultrasonic bath for 5 min. Then, 1 mL of the suspension was deposited onto a 9.1 cm² glass plate to obtain an even layer of the sample with a surface density of 1 mg/cm². After drying at 60 °C for 2 h, the plate was placed into the reactor, which was regulated at 25 °C. The relative humidity during the experiments was ca. 15%.

Before the kinetics experiment, the sample was UV irradiated for 1 h to decompose the compounds previously adsorbed on the catalyst surface during storage. The UV-LED, which was described above, was used as a UV source. After the pretreatment, 500 μL of gaseous CO under ambient pressure was injected into the reactor corresponding to a concentration of 1680 ppm. The oxidation of CO was investigated in the absence and presence of UV irradiation. In the former case, CO was oxidized without UV irradiation due to the thermal catalytic pathway, and the dark catalytic activity of the sample was evaluated. In the latter case, the UV-LED was turned on after the injection of CO, and the activity of the sample under UV irradiation was evaluated.

For both cases, the CO and CO_2 concentrations were calculated from the collected IR spectra, which were periodically recorded during the experiments. The calculation of CO was performed using spectral subtraction by minimizing the spectrum length at 2030–2240 cm⁻¹ [53], and the Beer-Lambert law at 2240–2450 cm⁻¹ was employed for CO_2 analysis. Typical kinetic plots for CO removal and CO_2 accumulation during the CO oxidation under dark conditions and under UV irradiation are shown in Fig. 3a and b, respectively. The initial rate of CO removal (W_{CO}) calculated by the linearization of the respective section of the CO kinetic plot was used to investigate the effects of the UV light, the support, the decomposition method of Pd(acac)₂, and the Pd content.

The photonic efficiency was estimated to evaluate the efficiency of incident UV light utilization. According to IUPAC recommendations [54], the photonic efficiency for CO oxidation can be expressed as follows:

$$\xi_{\text{CO}} = \frac{\frac{dN(\text{CO})}{dt}}{q_p^0} = \frac{(W_{\text{UV}}^0(\text{CO}) - W_{\text{dark}}^0(\text{CO})) \times 2.046 \times 10^{-10}}{S \int_{\lambda_1}^{\lambda_2} E_{n,p,\lambda}^0 d\lambda} \times 100\%$$

where ξ_{CO} is the photonic efficiency (%), $\frac{dN(\text{CO})}{dt}$ is the photocatalytic rate of CO oxidation (mol/s), q_p^0 is the incident photon flux (mol/s), $W_{\text{UV}}^0(\text{CO})$ and $W_{\text{dark}}^0(\text{CO})$ are the initial rates of CO oxidation under UV and in the dark, respectively (ppm/min), S is the area of a glass plate with the deposited photocatalyst ($S = 9.1 \text{ cm}^2$), $E_{n,p,\lambda}^0$ is the spectral photon irradiance ($\text{mol} \times \text{s}^{-1} \times \text{cm}^{-2} \times \text{nm}^{-1}$, see the insets in Fig. 1), and λ_1 and λ_2 are the wavelengths (315 and 390 nm) used for the integration of the spectral photon irradiance. The higher

wavelength (i.e., 390 nm) corresponds to the energy of 3.2 eV, which is equal to the band gap of the anatase form of TiO_2 .

3. Results and discussion

TiO_2 was modified with palladium to develop a highly active photocatalyst in CO oxidation under ambient conditions. Pd deposition was performed via thermal or photodecomposition of a metal-organic precursor, $\text{Pd}(\text{acac})_2$. Other supports, including ceria, silica, and alumina, were also investigated to emphasize the special features of titania. The effects of the preparation and the experimental parameters on the activity and characteristics of the catalysts are discussed below.

3.1. Effects of UV light and support

TiO_2 supported with noble metals can oxidize CO at room temperature. UV irradiation results in a substantial increase in the oxidation rate. Therefore, to check the effect of UV irradiation in this study correctly, the activity of the Pd-loaded catalysts was evaluated in the absence of UV irradiation (i.e., dark) at first, and then under UV irradiation. Non-semiconducting supports, SiO_2 and Al_2O_3 , were also employed to confirm the photocatalytic oxidation of CO with semiconducting supports, TiO_2 and CeO_2 .

The 2 wt.% Pd-loaded samples prepared via thermal decomposition of $\text{Pd}(\text{acac})_2$ at 210 °C were selected for these experiments. The TiO_2 support alone was also investigated to determine the effect of palladium. The results of the experiments are shown in Fig. 4.

No activity toward CO oxidation in the absence of UV irradiation was observed for pure TiO_2 . A low activity was observed after Pd deposition on the TiO_2 surface (i.e., 2Pd/ TiO_2 -210). The initial rate of CO oxidation was 8.8 ppm/min for 2Pd/ TiO_2 -210. The dark oxidation of CO over the Pd-loaded TiO_2 catalyst is due to a thermal catalytic pathway with the assistance of Pd.

Under UV irradiation of 10.4 mW/cm², TiO_2 completely oxidized CO to CO_2 according to the stoichiometry of this reaction, but the reaction rate was extremely low (0.7 ppm/min). By contrast, a very high activity was observed for the 2 wt.% Pd-loaded TiO_2 catalyst under UV irradiation. The initial rate of CO oxidation over 2Pd/ TiO_2 -210 was 38 ppm/min corresponding to a 4-fold increase in the activity compared

to the dark activity for this sample. The increase in the oxidation rate under UV irradiation is due to the photocatalytic oxidation pathway with the assistance of photogenerated charge carriers formed by the absorption of UV light. This statement is also supported by the results for the CeO_2 , SiO_2 - and Al_2O_3 -based samples. For the 2Pd/ CeO_2 -210 sample, which is based on the semiconducting support, the activity under UV irradiation was also higher than in the dark, but this effect was much lower compared to 2Pd/ TiO_2 -210. Typically, CeO_2 has a much lower activity in gas-phase photocatalytic oxidation compared to TiO_2 [55,56], which may explain the lower activity of 2Pd/ CeO_2 -210 in CO oxidation under UV irradiation. In contrast to the TiO_2 - and CeO_2 -based samples, no substantial difference in the rate of CO oxidation in the absence and presence of UV irradiation was observed for the 2Pd/ SiO_2 -210 and 2Pd/ Al_2O_3 -210 samples, which are based on the non-semiconducting supports, SiO_2 and Al_2O_3 (Fig. 4).

The results described above confirm that the photocatalytic oxidation of carbon monoxide occurs on the surface of TiO_2 -based catalysts. For pure TiO_2 , it is a very slow process. The deposition of palladium on the TiO_2 surface substantially increases the oxidation rate. The catalytic pathway due to thermal oxidation on the metal particles and the photocatalytic pathway due to the oxidation by highly active charged species formed under UV light can occur on the surface of TiO_2 supported with palladium. In this study, at a UV irradiance of 10.4 mW/cm², the contribution of the latter pathway at room temperature was much higher than of the former pathway.

3.2. Effect of the decomposition method

Two methods, namely, thermal decomposition by the calcination at the temperature of 210, 250 or 310 °C and photodecomposition by long-term UV irradiation, were employed to decompose $\text{Pd}(\text{acac})_2$ and deposit Pd nanoparticles on the TiO_2 surface. These methods can provide different distributions of Pd particles on the surface and different compositions of the metallic or oxidized forms of the deposited palladium. These characteristics affect the activity in CO oxidation.

Fig. 5 shows the effect of the decomposition method on the activity of TiO_2 catalysts supported with 2 wt.% Pd. The initial rate of CO oxidation over the 2Pd/ TiO_2 -P sample prepared via the photodecomposition of $\text{Pd}(\text{acac})_2$ absorbed on the TiO_2 surface was 17 ppm/min in the

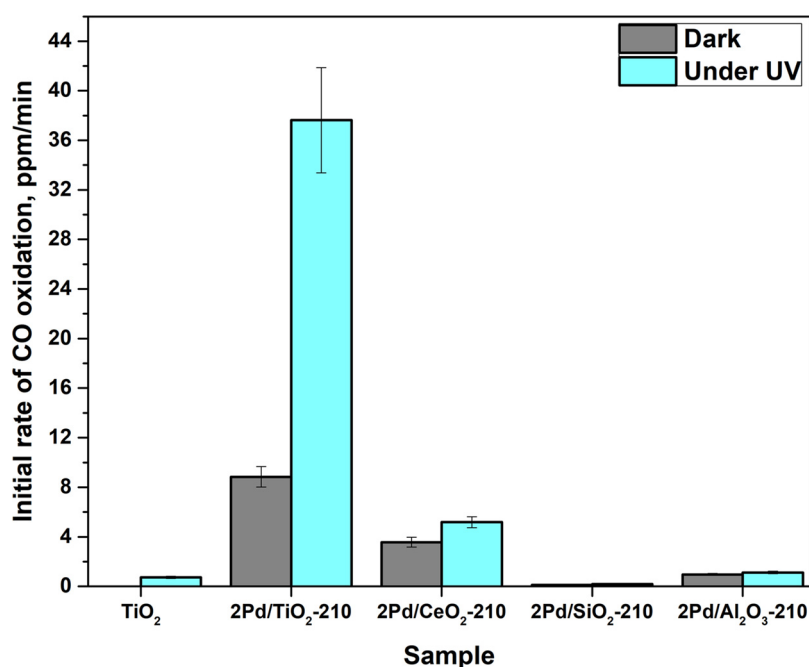


Fig. 4. CO oxidation rates for pure TiO_2 and the 2 wt.% Pd-loaded catalysts.

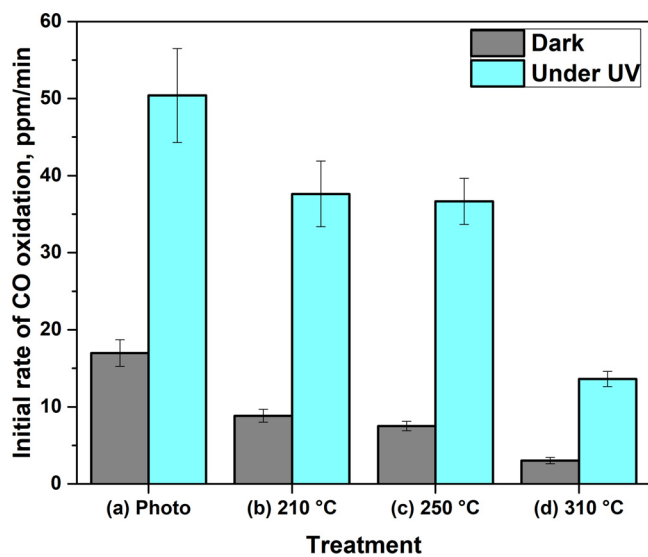


Fig. 5. CO oxidation rate for 2Pd/TiO₂-P (a), 2Pd/TiO₂-210 (b), 2Pd/TiO₂-250 (c), and 2Pd/TiO₂-310 (d).

absence of UV irradiation and 50 ppm/min under UV irradiation (Fig. 5a), which are substantially higher than the corresponding values for all the samples prepared via the calcination (Fig. 5b–d). This result indicates that the deposition of Pd on the TiO₂ surface via the photodecomposition method results in a higher CO oxidation activity compared to the thermal decomposition method. To elucidate the effect of the decomposition method, the surface composition and morphology of these samples were investigated by XPS and TEM analyses.

Fig. 6 shows the photoelectron Pd3d spectral regions measured for the reference samples and the TiO₂ catalysts supported with palladium. Palladium oxide (PdO), Pd(acac)₂ precursor, and Pd foil were used as the reference samples (Fig. 6a) because they included palladium in different charge states (i.e., Pd⁰ and Pd²⁺) and different coordination environments (i.e., PdO and Pd(acac)₂), which allow us to correctly identify the Pd states in the studied catalysts.

The Pd3d spectral region for the 2Pd/TiO₂-210 catalyst (Fig. 6b) was fitted by two doublet components with BE(Pd3d_{5/2}) values of 335.5 and 336.6 eV, which, according to the reference samples, can be attributed to metallic palladium and PdO, respectively [57]. This result

Table 2
Surface content of different Pd forms evaluated from XPS data for the Pd-loaded catalysts.

Sample	Surface content, %		
	Pd(acac) ₂	Pd ⁰	PdO
2Pd/TiO ₂ -210	0	35	65
2Pd/TiO ₂ -P	11	47	42
2Pd/TiO ₂ -P (after reaction)	8	53	39

indicates that even at a low temperature, 210 °C, Pd(acac)₂ is completely decomposed on the TiO₂ surface with the deposition of metallic palladium (Pd⁰) and palladium oxide (PdO). By contrast, the Pd3d spectral region for the 2Pd/TiO₂-P catalyst prepared via the photodecomposition of Pd(acac)₂ had an additional doublet component with a BE(Pd3d_{5/2}) of 338.1 eV, which can be attributed to the Pd²⁺ state in the Pd(acac)₂ precursor. This result indicates that, in the case of the photodecomposition method, a portion of Pd(acac)₂ remains in the initial state on the TiO₂ surface even after long-term UV irradiation.

The surface content of different Pd forms was evaluated from the intensities of the corresponding doublet components. The results are shown in Table 2. The thermally treated catalyst 2Pd/TiO₂-210 had only 35% of metallic palladium (Pd⁰). The rest of Pd (65%) was in the form of palladium oxide (PdO). This result is surprising because Xie et al. [45] detected metallic Pd nanoparticles only during low-temperature (ca. 200 °C) decomposition of Pd(acac)₂ on the SiO₂ surface. A large amount of PdO, in the case of the TiO₂-based catalyst, is due to specific features of TiO₂ as a support. TiO₂ may have a strong interaction with a Pd precursor resulting in the formation of PdO even in the presence of a reducing agent. For example, in our previous study [43], we synthesized Pd/TiO₂ catalysts via the reduction of a PdCl₂ precursor with a three-fold molar excess of NaBH₄, but the complete reduction of PdCl₂ to Pd⁰ was not achieved. According to the XPS data, the Pd⁰/PdO atomic ratio was 7:5. At the same time, metallic Pt and Au particles were only observed on the TiO₂ surface in the chemical reduction of H₂PtCl₆ and HAuCl₄ by the same way.

The photodecomposition method resulted in a higher content of Pd⁰ (47%) and a lower content of PdO (42%) but, as mentioned above, a significant portion of Pd was in the initial form of Pd(acac)₂ (11%). The incomplete decomposition of Pd(acac)₂ was probably due to insufficient time of UV treatment. It can be expected that after long exposure to UV

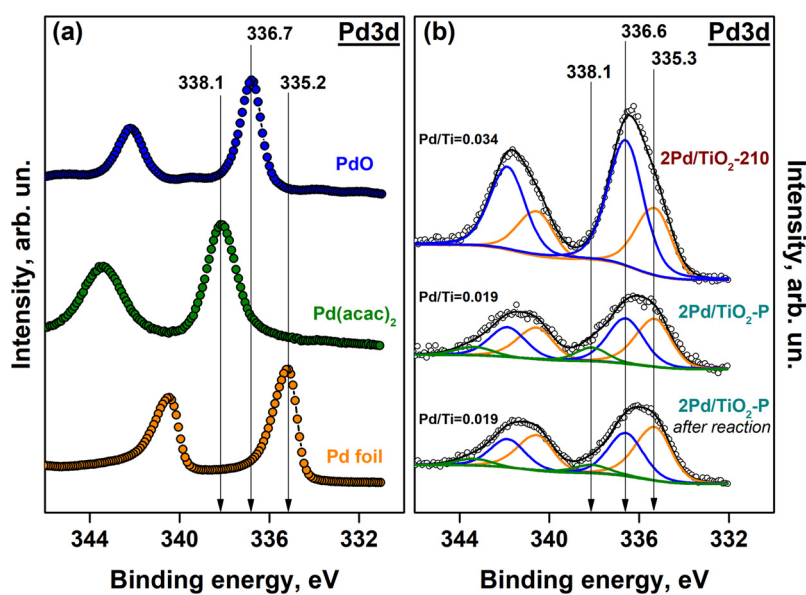


Fig. 6. Photoelectron Pd3d spectral regions for the reference samples (a) and the TiO₂ catalysts supported with 2 wt.% of Pd (b).

irradiation the $\text{Pd}(\text{acac})_2$ would be completely decomposed. XPS data for the 2Pd/TiO₂-P sample after CO oxidation shows a decrease in the $\text{Pd}(\text{acac})_2$ and PdO content with a simultaneous increase in Pd^0 content (Table 2).

The deposition of Pt in the forms of Pt^0 , Pt^{2+} , Pt^{4+} on TiO₂ was shown by Vorontsov et al. [40] resulting in a substantial increase in the CO photocatalytic oxidation rate compared to TiO₂ alone. The metallic form of Pt had the highest effect on the photocatalytic activity. The same situation is likely observed for other noble metals. Therefore, more metallic palladium may be the reason for higher activity for the catalyst prepared via the photodecomposition method compared to the thermal decomposition.

It is important to note that the treatment of Pd-loaded catalysts in a reducing atmosphere (e.g., calcination in a stream of hydrogen) was not employed to avoid the influence of TiO₂ reduction on the photocatalytic activity of the catalysts. The reduced sites are the sites for the recombination of photogenerated charge carriers that are well known to result in a decrease in the photocatalytic activity of TiO₂ in the oxidation of VOCs under UV irradiation. Investigation of the TiO₂ reduction treatment on its activity in the photocatalytic oxidation of CO is beyond the scope of this study.

In addition to the charge state, the size of the noble metal particles and their distribution on the support surface are key factors. TEM analysis was employed to evaluate the morphology of deposited Pd particles. The uniformly distributed 5–15 nm agglomerates of Pd and PdO nanoparticles were detected on the surface of 2Pd/TiO₂-P prepared via the photodecomposition method (Fig. 7). The formation of large particles is typical for the photodeposition methods because the sites for the liberation of photogenerated electrons on the TiO₂ surface simultaneously act as sites for the metal reduction resulting in the crystallization and growth of particles in the certain places [39]. The presence of large Pd particles on the TiO₂ surface explains the lower Pd/Ti atomic ratio in the photoelectron spectra for the 2Pd/TiO₂-P catalyst compared to 2Pd/TiO₂-210, as shown in Fig. 6b. In addition to the agglomerates, small Pd clusters can also be detected on the 2Pd/TiO₂-P surface.

In the case of 2Pd/TiO₂-210 prepared via the calcination at 210 °C, no Pd nanoparticles were detected in the TEM photos (Fig. 8). At the same time, EDX spectra revealed the peak corresponding to palladium. This result indicates that palladium on the surface of 2Pd/TiO₂-210 photocatalyst was in the form of clusters in a size less than 0.5 nm.

Wang et al. [44] published similar results for Pd/TiO₂ prepared via thermal treatment of $\text{Pd}(\text{acac})_2$ deposited on the TiO₂ surface.

An optimal size of the metal particles for fast interface electron transfer and high photocatalytic activity exists. Very small metal particles may have a sub-optimal Fermi level position, which hinders the transfer of photogenerated electrons from TiO₂ onto the metal due to the high Fermi level in the small metal particles and, consequently, the overall process [39,41]. Therefore, different sizes of Pd particles may also be a reason for different photocatalytic activities of the catalysts prepared via thermal and photodecomposition methods.

The data in Fig. 5 also allow for the evaluation of the effect of the calcination temperature during the thermal decomposition method. No substantial difference in the CO oxidation rate in the dark and under UV irradiation was observed for the 2Pd/TiO₂-210 and 2Pd/TiO₂-250 catalysts calcined at 210 and 250 °C, respectively. However, the initial rate of CO oxidation for the 2Pd/TiO₂-310 sample calcined at 310 °C was 3.0 ppm/min in the absence of UV irradiation and 13.6 ppm/min under UV irradiation. These values were much lower than the rates for 2Pd/TiO₂-210 and 2Pd/TiO₂-250, corresponding to a substantial decrease in the activity at a high calcination temperature. Such behavior may be due to the oxidation of Pd to PdO in the air at a high temperature and a decrease in the content of metallic Pd.

To summarize the characterization data, the photodecomposition method results in Pd deposition on the TiO₂ surface mainly in the forms of Pd^0 and PdO , and the content of Pd^0 is higher than for the thermal decomposition method. The Pd particles of sizes 5–15 nm are deposited on the TiO₂ surface during the photodecomposition, while in the case of the thermal decomposition no Pd nanoparticles are observed. The photodecomposition method results in a 1.4 times higher activity in CO oxidation under UV irradiation compared to the activity from the thermal decomposition method.

3.3. Effect of the Pd content

In many photocatalytic processes with supporting metals, the activity has a domed dependence on the metal content. In our previous study [43], we observed the dependence of CO photocatalytic oxidation over the M/TiO₂ catalysts prepared via the chemical reduction of chlorinated precursors. The main reason for such dependence was the size of the metal particles, which increased as the metal content increased, and their agglomeration. By contrast, the activity for the

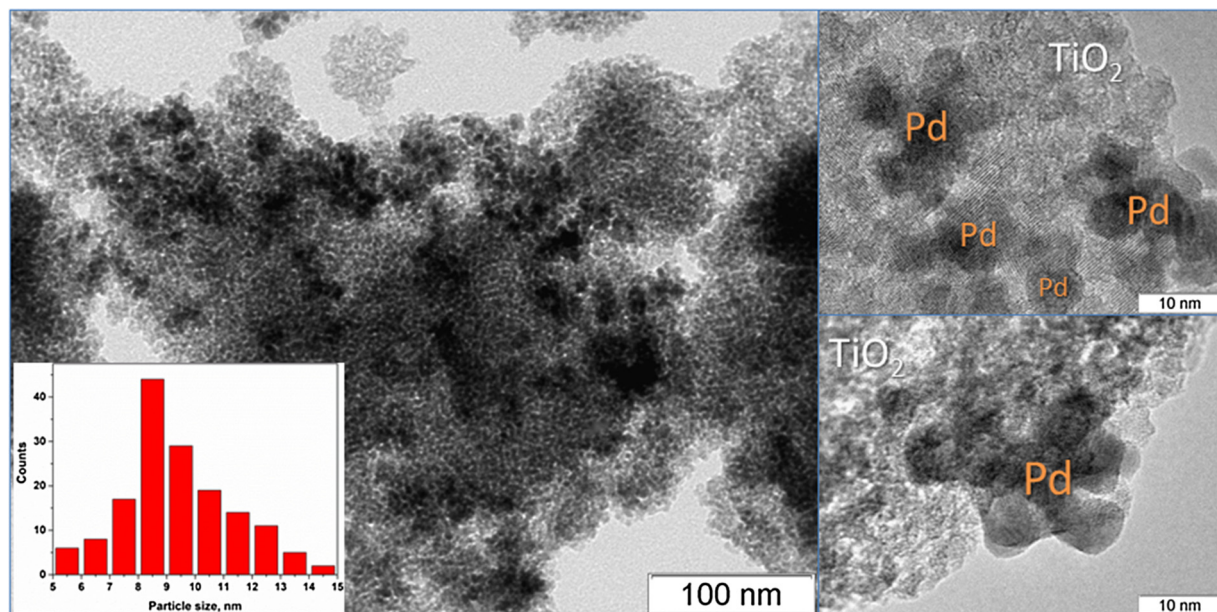


Fig. 7. TEM photographs for the 2Pd/TiO₂-P catalyst prepared via photodecomposition method.

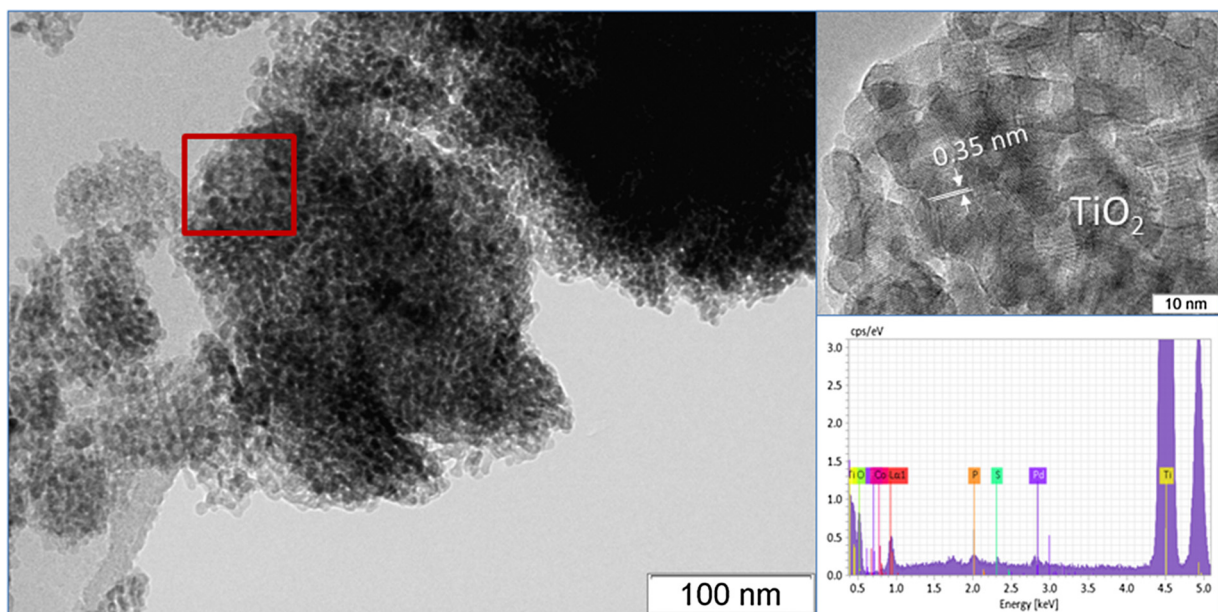


Fig. 8. TEM photographs for the 2Pd/TiO₂-210 catalyst prepared via thermal decomposition method.

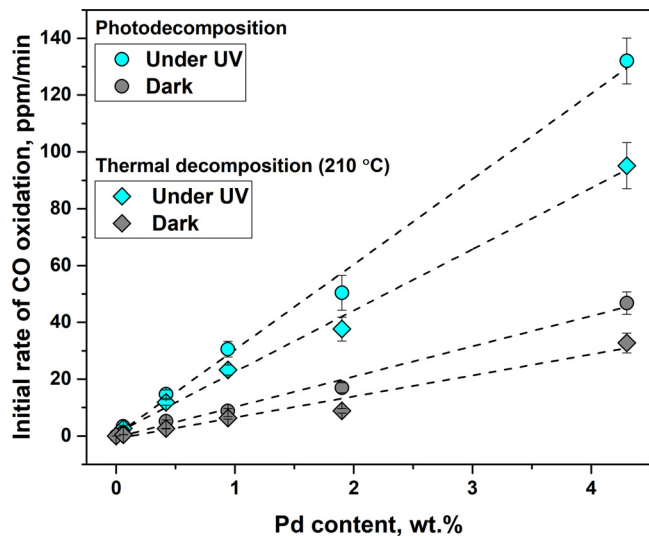


Fig. 9. Dependence of the CO oxidation rate on the Pd content in the Pd/TiO₂ catalysts prepared via thermal and photodecomposition methods.

catalyst prepared via the decomposition of Pd(acac)₂ monotonically increased as the Pd content increased both in the absence and presence of UV irradiation (Fig. 9). The data were well fitted by a linear curve for all cases.

Such dependence may be explained by the stability of size and distribution of Pd particles when increasing the Pd content. To verify this assumption, the catalysts were investigated by pulse CO chemisorption and TEM analysis.

Due to a high number of Pd clusters on the surface of the Pd-loaded catalyst, analysis of their dispersion using CO chemisorption measurements is preferable compared to TEM analysis because it can give an integral characteristic for the particles with different sizes, including very small particles. Before the chemisorption measurements, the catalysts were reduced under mild conditions to purify the catalyst surface and reduce all the Pd forms to metallic palladium. The estimated data for the dispersion of Pd particles on the surface of 2 and 4 wt.% Pd-loaded catalysts are shown in Table 3.

The dispersion for the catalysts prepared via thermal decomposition

of Pd(acac)₂ was ca. 2 times higher than from the photodecomposition method, which agrees completely with the TEM data. For both decomposition methods, the dispersion of Pd particles slightly decreased as the Pd content increased from 1.9 to 4.3 wt.%. This result indicates that the number of Pd particles increased as the Pd content increased, but their distribution on the TiO₂ surface were similar to that at a low Pd content, which can explain the linear increase in activity over the whole range of Pd content in this study. To illustrate stability of the particle distribution, Fig. 10 shows TEM photos for the 4 wt.% Pd-loaded catalyst prepared via the photodecomposition method. No substantial aggregation of the Pd particles was observed at a high Pd content. The uniformly distributed 8–20 nm agglomerates were detected on the surface of 4Pd/TiO₂-P. A shift of size distribution to the range of higher values was observed for this sample compared to the 2 wt.% Pd-loaded catalyst (Fig. 7).

Therefore, the decomposition of Pd(acac)₂ is an efficient method for the deposition of uniformly distributed Pd nanoparticles on the TiO₂ surface even at a high Pd content, which results in a high activity. It is important to note that the subsequent increase in the Pd content, to higher than 4 wt.%, was difficult due to crystallization of the Pd precursor during the evaporation of solvent, causing the formation of large particles on the TiO₂ surface. The consecutive procedures of Pd deposition in a smaller content were required for solving this problem. Additionally, a very high content of noble metal has low importance in practice due to the high cost of such catalyst. These circumstances were the reasons that Pd-loaded catalysts were studied only in the range of 0.1–4 wt.%.

3.4. Photonic efficiency

The photonic efficiency was estimated for 4Pd/TiO₂-P as the most active catalyst to evaluate the efficiency of incident UV light use. The initial rate of CO oxidation for this catalyst was 47 and 132 ppm/min in the absence and presence of UV irradiation, respectively. The rate of photocatalytic oxidation can be estimated as a difference in these values. This corresponds to an assumption that UV irradiation increases the reaction rate of CO oxidation due to the photocatalytic pathway without suppressing the thermal catalytic pathway. According to the expression described in Section 2.4, the photonic efficiency of 4Pd/TiO₂-P is 5.9%, which is a high value. For example, the rate of CO oxidation over the 1 wt.% Pt/TiO₂ catalyst, which was the most active

Table 3

Pd dispersion from the CO chemisorption data.

Sample	Decomposition method	Experimental Pd content, wt.%	Dispersion of Pd particles, D_{Pd} , %	TEM particles size, nm
2Pd/TiO ₂ -210	Thermal (210 °C)	1.9	54.0	< 0.5
4Pd/TiO ₂ -210	Thermal (210 °C)	4.3	50.2	< 1
2Pd/TiO ₂ -P	Photo	1.9	28.6	5–15
4Pd/TiO ₂ -P	Photo	4.3	24.3	8–20

catalysts among the 0.01–4 wt.% Pt-, Pd-, and Au-loaded catalysts synthesized via the chemical reduction of chlorinated precursors, under the same conditions was 11.6 and 44 ppm/min in the absence and presence of UV irradiation, respectively [43], corresponding to a photonic efficiency of only 2.3%.

It is important to note that the value of the photonic efficiency for 4Pd/TiO₂-P is a low estimate because we used the difference between the rates in the absence and presence of UV irradiation. If we consider the rate under UV irradiation only, the value of the photonic efficiency would be 9.1%.

3.5. Future prospects

In this study, we present the effect of two methods for decomposition of palladium acetylacetone (Pd(acac)₂) precursor using thermal or UV treatment on the formation of Pd nanoparticles on the TiO₂ surface and the activity of Pd-loaded catalysts in the oxidation of CO under dark and UV conditions. It is important to note that similar results were also observed for another Pd precursor, palladium acetate (Pd(OAc)₂). For example, the effect of the decomposition method on the activity of 2 wt.% Pd/TiO₂ catalysts prepared from Pd(OAc)₂ during the CO oxidation under the same conditions can be found in the SI section. These results lead to suppose that the decomposition of metal-organic precursors has good promise for the preparation of metal/TiO₂ photocatalysts for air purification. The following advantages may be achieved:

- 1) No chlorine atoms, which could otherwise remain on the photocatalyst surface and be the sites for the recombination of photo-generated charge carriers, decreasing the quantum efficiency of the process;
- 2) No loss in the specific surface area of the photocatalyst, resulting

from high-temperature calcination, because the decomposition of the precursor may be achieved at a low temperature;

- 3) No need of a reducing agent (or reducing atmosphere) during the synthesis, which can partially reduce the TiO₂ surface, because the decomposition of these types of precursors in the air can result in the formation of a metal mainly in the metallic form.

The main drawback of palladium as a metal for TiO₂ modification is the formation of a large amount of PdO due to the strong interaction with the TiO₂ support. At the same time, the metallic form is preferable because it usually gives a higher photocatalytic activity. From this point of view, the platinum attracts greater attention because the complete reduction of the Pt precursor to metallic Pt can be easily achieved. Therefore, the photodecomposition of the Pt complexes, such as Pt(acac)₂, Pt(NH₃)₂(NO₂)₂, or bimetallic complexes, on the irradiated surface of TiO₂ holds promise for future work to prepare highly active metal-TiO₂ photocatalysts.

4. Conclusions

Two methods, namely, the thermal decomposition of Pd(acac)₂ by the calcination at the temperature of 210–310 °C and the photodecomposition of Pd(acac)₂ by long-term UV irradiation, are employed to synthesize TiO₂, CeO₂, SiO₂, or Al₂O₃-based catalysts supported with palladium for CO oxidation.

All synthesized catalysts completely oxidize CO to CO₂ at room temperature. UV-LED irradiation with a total irradiance of 10.4 mW/cm² in the UVA region increases the CO oxidation rate up to 5 times for TiO₂ or 1.5 times for CeO₂ compared to dark catalytic oxidation. By contrast, no substantial difference in the CO oxidation rate is observed for the SiO₂ and Al₂O₃ non-semiconducting supports in the absence and presence of UV irradiation, which confirms the photocatalytic oxidation

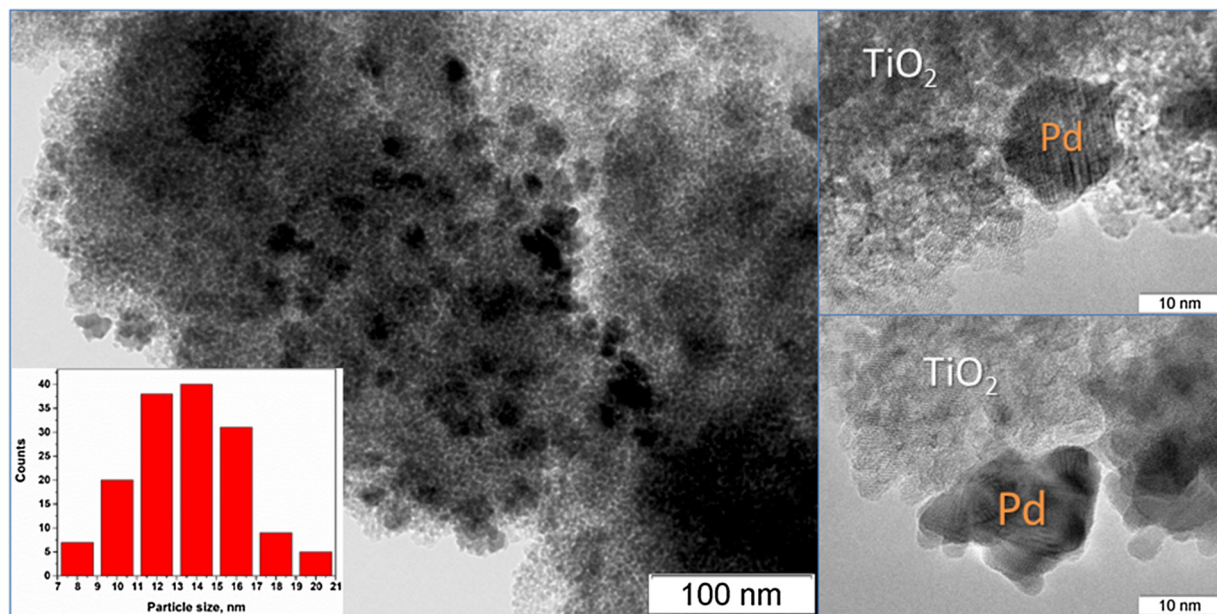


Fig. 10. TEM photographs for the 4Pd/TiO₂-P catalyst prepared via photodecomposition method.

of carbon monoxide on the surface of TiO_2 supported with palladium.

Both employed methods result in the deposition of Pd on the TiO_2 surface mainly in the metallic (Pd^0) and oxidized (PdO) forms of palladium, and the Pd^0 content is higher for the photodecomposition method. 5–20 nm particles and small clusters are deposited on the TiO_2 surface during photodecomposition, while in the case of the thermal decomposition, no Pd nanoparticles are observed. The activity toward CO oxidation under UV irradiation for the photodecomposition method is 1.4 times higher compared to that for the thermal decomposition method. Additionally, the increase in the calcination temperature from 210 to 310 °C during the thermal decomposition results in a strong decrease in the CO oxidation rate.

In the range of Pd content from 0.1 to 4 wt.%, the rate of CO oxidation under UV irradiation as well as under the dark condition monotonically increases as the Pd content increases due to the stability of a high dispersion of Pd particles even at a high Pd content. The maximum value of the photonic efficiency during CO photocatalytic oxidation over the synthesized catalysts is 5.9%.

Acknowledgements

This study was funded by Russian Science Foundation according to the research project No.17-73-10342.

Appendix A. Supplementary data

Supplementary material related to this article can be found, in the online version, at doi:<https://doi.org/10.1016/j.apcatb.2018.04.074>.

References

- World Health Organization, <http://www.who.int/mediacentre/news/releases/2016/air-pollution-estimates/en/> (accessed 03.04.17).
- R. Andreozzi, Advanced oxidation processes (AOP) for water purification and recovery, *Catal. Today.* 53 (1999) 51–59, [http://dx.doi.org/10.1016/S0920-5861\(99\)00102-9](http://dx.doi.org/10.1016/S0920-5861(99)00102-9).
- W.H. Glaze, J.-W. Kang, D.H. Chapin, The chemistry of water treatment processes involving ozone, hydrogen peroxide and ultraviolet radiation, *Ozone Sci. Eng.* 9 (1987) 335–352, <http://dx.doi.org/10.1080/01919518708552148>.
- G.P. Anipitsakis, D.D. Dionysiou, Degradation of organic contaminants in water with sulfate radicals generated by the conjunction of peroxyomonosulfate with cobalt, *Environ. Sci. Technol.* 37 (2003) 4790–4797, <http://dx.doi.org/10.1021/es0263792>.
- J. Sharma, I.M. Mishra, D.D. Dionysiou, V. Kumar, Oxidative removal of bisphenol a by UV-C/peroxyomonosulfate (PMS): kinetics, influence of co-existing chemicals and degradation pathway, *Chem. Eng. J.* 276 (2015) 193–204, <http://dx.doi.org/10.1016/j.cej.2015.04.021>.
- J. Rodriguez-Chueca, C. Amor, T. Silva, D.D. Dionysiou, G. Li Puma, M.S. Lucas, J.A. Peres, Treatment of winery wastewater by sulphate radicals: HSO_5^- /transition metal/UV-A LEDs, *Chem. Eng. J.* 310 (2017) 473–483, <http://dx.doi.org/10.1016/j.cej.2016.04.135>.
- U.I. Gaya, A.H. Abdullah, Heterogeneous photocatalytic degradation of organic contaminants over titanium dioxide: a review of fundamentals, progress and problems, *J. Photochem. P. Photochem. Rev.* 9 (2008) 1–12, <http://dx.doi.org/10.1016/j.jphotochemrev.2007.12.003>.
- Y. Paz, Photocatalytic treatment of air, *Adv. Chem. Eng.* 36 (2009) 289–336, [http://dx.doi.org/10.1016/S0065-2377\(09\)00408-6](http://dx.doi.org/10.1016/S0065-2377(09)00408-6).
- Y. Paz, Application of TiO_2 photocatalysis for air treatment: patents' overview, *Appl. Catal. B Environ.* 99 (2010) 448–460, <http://dx.doi.org/10.1016/j.apcatb.2010.05.011>.
- T.M. Fujimoto, M. Ponczek, U.L. Rochetto, R. Landers, E. Tomaz, Photocatalytic oxidation of selected gas-phase VOCs using UV light, TiO_2 , and TiO_2/Pd , *Environ. Sci. Pollut. Res.* 24 (2017) 6390–6396, <http://dx.doi.org/10.1007/s11356-016-6494-7>.
- G.-M. Zuo, Z.-X. Cheng, G.-W. Li, W.-P. Shi, T. Miao, Study on photolytic and photocatalytic decontamination of air polluted by chemical warfare agents (CWAs), *Chem. Eng. J.* 128 (2007) 135–140, <http://dx.doi.org/10.1016/j.cej.2006.10.006>.
- P.A. Kolinko, D.V. Kozlov, A.V. Vorontsov, S.V. Preis, Photocatalytic oxidation of 1,1-dimethyl hydrazine vapours on TiO_2 : FTIR in situ studies, *Catal. Today.* 122 (2007) 178–185, <http://dx.doi.org/10.1016/j.cattod.2007.01.029>.
- D. Sharabi, Y. Paz, Preferential photodegradation of contaminants by molecular imprinting on titanium dioxide, *Appl. Catal. B Environ.* 95 (2010) 169–178, <http://dx.doi.org/10.1016/j.apcatb.2009.12.024>.
- F. Moulis, J. Krýsa, Photocatalytic degradation of several VOCs (n-hexane, n-butyl acetate and toluene) on TiO_2 layer in a closed-loop reactor, *Catal. Today.* 209 (2013) 153–158, <http://dx.doi.org/10.1016/j.cattod.2012.10.017>.
- D. Selishchev, D. Kozlov, Photocatalytic oxidation of diethyl sulfide vapor over TiO_2 -based composite photocatalysts, *Molecules* 19 (2014) 21424–21441, <http://dx.doi.org/10.3390/molecules191221424>.
- A.H. Mamaghani, F. Haghhighat, C.-S. Lee, Photocatalytic oxidation technology for indoor environment air purification: the state-of-the-art, *Appl. Catal. B Environ.* 203 (2017) 247–269, <http://dx.doi.org/10.1016/j.apcatb.2016.10.037>.
- Y. Boyjoo, H. Sun, J. Liu, V.K. Pareek, S. Wang, A review on photocatalysis for air treatment: from catalyst development to reactor design, *Chem. Eng. J.* 310 (2017) 537–559, <http://dx.doi.org/10.1016/j.cej.2016.06.090>.
- P.A. Kolinko, D.V. Kozlov, Products distribution during the gas phase photocatalytic oxidation of ammonia over the various titania based photocatalysts, *Appl. Catal. B Environ.* 90 (2009) 126–131, <http://dx.doi.org/10.1016/j.apcatb.2009.03.001>.
- M.C. Canela, R.M. Alberici, W.F. Jardim, Gas-phase destruction of H_2S using TiO_2 /UV-VIS, *J. Photochem. Photobiol. A* 112 (1998) 73–80, [http://dx.doi.org/10.1016/S1010-6030\(97\)00261-X](http://dx.doi.org/10.1016/S1010-6030(97)00261-X).
- S. Kataoka, E. Lee, M.I. Tejedor-Tejedor, M.A. Anderson, Photocatalytic degradation of hydrogen sulfide and in situ FT-IR analysis of reaction products on surface of TiO_2 , *Appl. Catal. B Environ.* 61 (2005) 159–163, <http://dx.doi.org/10.1016/j.apcatb.2005.04.018>.
- I. Sopyan, Kinetic analysis on photocatalytic degradation of gaseous acetaldehyde, ammonia and hydrogen sulfide on nanosized porous TiO_2 films, *Sci. Technol. Adv. Mater.* 8 (2007) 33–39, <http://dx.doi.org/10.1016/j.stam.2006.10.004>.
- Federal state statistics service (Rosstat), Environmental Protection in Russia, Statistics book, Moscow, 2014.
- D.S. Selishchev, I.P. Karaseva, V.V. Uvaev, D.V. Kozlov, V.N. Parmon, Effect of preparation method of functionalized textile materials on their photocatalytic activity and stability under UV irradiation, *Chem. Eng. J.* 224 (2013) 114–120, <http://dx.doi.org/10.1016/j.cej.2012.12.003>.
- D.S. Selishchev, N.S. Kolobov, A.A. Pershin, D.V. Kozlov, TiO_2 mediated photocatalytic oxidation of volatile organic compounds: formation of CO as a harmful by-product, *Appl. Catal. B Environ.* 200 (2017) 503–513, <http://dx.doi.org/10.1016/j.apcatb.2016.07.044>.
- M. Valden, X. Lai, D.W. Goodman, Onset of catalytic activity of gold clusters on titania with the appearance of nonmetallic properties, *Science* 281 (1998) 1647–1650, <http://dx.doi.org/10.1126/science.281.5383.1647>.
- G.C. Bond, D.T. Thompson, Catalysis by Gold, *Catal. Rev.* 41 (1999) 319–388, <http://dx.doi.org/10.1081/CR-100101171>.
- G.R. Bamwenda, S. Tsubota, T. Nakamura, M. Haruta, The influence of the preparation methods on the catalytic activity of platinum and gold supported on TiO_2 for CO oxidation, *Catal. Letters* 44 (1997) 83–87, <http://dx.doi.org/10.1023/A:1018925008633>.
- N. Li, Q.-Y. Chen, L.-F. Luo, W.-X. Huang, M.-F. Luo, G.-S. Hu, J.-Q. Lu, Kinetic study and the effect of particle size on low temperature CO oxidation over Pt/TiO_2 catalysts, *Appl. Catal. B Environ.* 142–143 (2013) 523–532, <http://dx.doi.org/10.1016/j.apcatb.2013.05.068>.
- D.A. Svititskiy, L.S. Kibis, A.I. Stadnichenko, S.V. Koscheev, V.I. Zaikovskii, A.I. Boronin, Highly oxidized platinum nanoparticles prepared through radio-frequency sputtering: thermal stability and reaction probability towards CO, *ChemPhysChem.* 16 (2015) 3318–3324, <http://dx.doi.org/10.1002/cphc.201500546>.
- O. Rosseler, A. Louvet, V. Keller, N. Keller, Enhanced CO photocatalytic oxidation in the presence of humidity by tuning composition of Pd-Pt bimetallic nanoparticles supported on TiO_2 , *Chem. Commun.* 47 (2011) 5331–5333, <http://dx.doi.org/10.1039/c1cc10660k>.
- H. Einaga, A. Ogata, S. Futamura, T. Ibusuki, The stabilization of active oxygen species by Pt supported on TiO_2 , *Chem. Phys. Lett.* 338 (2001) 303–307, [http://dx.doi.org/10.1016/S0009-2614\(01\)00296-2](http://dx.doi.org/10.1016/S0009-2614(01)00296-2).
- S. Hwang, M.C. Lee, W. Choi, Highly enhanced photocatalytic oxidation of CO on titania deposited with Pt nanoparticles: kinetics and mechanism, *Appl. Catal. B Environ.* 46 (2003) 49–63, [http://dx.doi.org/10.1016/S0926-3373\(03\)00162-0](http://dx.doi.org/10.1016/S0926-3373(03)00162-0).
- G. Karakas, P. Yetisimyan, Room temperature photocatalytic oxidation of carbon monoxide over $\text{Pd}/\text{TiO}_2\text{-SiO}_2$ catalysts, *Top. Catal.* (2013) 1883–1891, <http://dx.doi.org/10.1007/s11244-013-0124-0>.
- O. Rosseler, C. Ulhaq-Bouillet, A. Bonnefont, S. Pronkin, E. Savinova, A. Louvet, V. Keller, N. Keller, Structural and electronic effects in bimetallic PdPt nanoparticles on TiO_2 for improved photocatalytic oxidation of CO in the presence of humidity, *Appl. Catal. B Environ.* 166 (2015) 381–392, <http://dx.doi.org/10.1016/j.apcatb.2014.12.001>.
- F. Bosc, A. Ayral, N. Keller, V. Keller, Room temperature visible light oxidation of CO by high surface area rutile TiO_2 -supported metal photocatalyst, *Appl. Catal. B Environ.* 69 (2007) 133–137, <http://dx.doi.org/10.1016/j.apcatb.2006.06.004>.
- J. Liu, R. Si, H. Zheng, Q. Geng, W. Dai, X. Chen, X. Fu, The promoted oxidation of CO induced by the visible-light response of Au nanoparticles over Au/TiO_2 , *Catal. Commun.* 26 (2012) 136–139, <http://dx.doi.org/10.1016/j.catcom.2012.05.011>.
- X.-Q. Deng, B. Zhu, X.-S. Li, J.-L. Liu, X. Zhu, A.-M. Zhu, Visible-light photocatalytic oxidation of CO over plasmonic Au/TiO_2 : unusual features of oxygen plasma activation, *Appl. Catal. B Environ.* 188 (2016) 48–55, <http://dx.doi.org/10.1016/j.apcatb.2016.01.055>.
- H. Chen, P. Li, N. Umezawa, H. Abe, J. Ye, K. Shiraishi, A. Ohta, S. Miyazaki, Bonding and energy alignment at metal/ TiO_2 interfaces: a density functional theory study, *J. Phys. Chem. C* 120 (2016) 5549–5556, <http://dx.doi.org/10.1021/acs.jpcc.5b12681> *acs.jpcc.5b12681*.
- T. Tanaka, J. Ohyama, K. Teramura, Y. Hitomi, Formation mechanism of metal nanoparticles studied by XAFS spectroscopy and effective synthesis of small metal nanoparticles, *Catal. Today.* 183 (2012) 108–118, <http://dx.doi.org/10.1016/j.cattod.2011.09.003>.

[40] A.V. Vorontsov, E.N. Savinov, J. Zhensheng, Influence of the form of photo-deposited platinum on titania upon its photocatalytic activity in CO and acetone oxidation, *J. Photochem. Photobiol. A Chem.* 125 (1999) 113–117, [http://dx.doi.org/10.1016/S1010-6030\(99\)00073-8](http://dx.doi.org/10.1016/S1010-6030(99)00073-8).

[41] M. Sadeghi, W. Liu, T.-G. Zhang, P. Stavropoulos, B. Levy, Role of photoinduced charge carrier separation distance in heterogeneous photocatalysis: oxidative degradation of CH_3OH vapor in contact with Pt/TiO_2 and cofumed $\text{TiO}_2-\text{Fe}_2\text{O}_3$, *J. Phys. Chem.* 100 (1996) 19466–19474, <http://dx.doi.org/10.1021/JP961335Z>.

[42] E.A. Kozlova, T.P. Lyubina, M.A. Nasalevich, A.V. Vorontsov, A.V. Miller, V.V. Kaichev, V.N. Parmon, Influence of the method of platinum deposition on activity and stability of Pt/TiO_2 photocatalysts in the photocatalytic oxidation of dimethyl methylphosphonate, *Catal. Commun.* 12 (2011) 597–601, <http://dx.doi.org/10.1016/j.catcom.2010.12.007>.

[43] N.S. Kolobov, D.A. Svintitskiy, E.A. Kozlova, D.S. Selishchev, D.V. Kozlov, UV-LED photocatalytic oxidation of carbon monoxide over TiO_2 supported with noble metal nanoparticles, *Chem. Eng. J.* 314 (2017) 600–611, <http://dx.doi.org/10.1016/j.cej.2016.12.018>.

[44] Z. Wang, B. Li, M. Chen, W. Weng, H. Wan, Size and support effects for CO oxidation on supported Pd catalysts, *Sci. China Chem.* 53 (2010) 2047–2056, <http://dx.doi.org/10.1007/s11426-010-4109-6>.

[45] Y. Xie, B. Li, W. Weng, Y. Zheng, K. Zhu, N. Zhang, C. Huang, H. Wan, Mechanistic aspects of formation of sintering-resistant palladium nanoparticles over SiO_2 prepared using $\text{Pd}(\text{acac})_2$ as precursor, *Appl. Catal. A Gen.* 504 (2015) 179–186, <http://dx.doi.org/10.1016/j.apcata.2014.12.008>.

[46] N.S. Kolobov, D.S. Selishchev, A.V. Bukhtiyarov, A.I. Gubanov, D.V. Kozlov, UV-LED photocatalytic oxidation of CO over the Pd/TiO_2 catalysts synthesized by the decomposition of $\text{Pd}(\text{acac})_2$, *Mater. Today Proc.* 4 (2017) 11356–11359, <http://dx.doi.org/10.1016/j.matpr.2017.09.008>.

[47] A.M.T. Silva, B.F. Machado, H.T. Gomes, J.L. Figueiredo, G. Dražić, J.L. Faria, Pt nanoparticles supported over Ce–Ti–O: the solvothermal and photochemical approaches for the preparation of catalytic materials, *J. Nanoparticle Res.* 12 (2010) 121–133, <http://dx.doi.org/10.1007/s11051-009-9584-3>.

[48] S. Dadsetan, S. Baghshahi, S. Mohammad, M. Hadavi, Photodeposition of Pd nanoparticles on TiO_2 using sacrificial organic alcohols, *J. Aust. Ceram. Soc.* 54 (2018) 383–388, <http://dx.doi.org/10.1007/s41779-017-0163-2>.

[49] S.P. Khranenko, S.V. Korenev, A.I. Gubanov, Method of producing beta-diketonate of palladium (and) or copper (II), RU 2433114, 2010.

[50] J.F. Moulder, W.F. Stickle, P.E. Sobol, K.D. Bomben, *Handbook of X-Ray Photoelectron Spectroscopy*, Perkin-Elmer Corp, Eden Prairie, Minnesota, USA, 1992.

[51] D.A. Bulushev, M. Zacharska, A.S. Lisitsyn, O.Y. Podyacheva, F.S. Hage, Q.M. Ramasse, U. Bangert, L.G. Bulusheva, Single atoms of Pt-group metals stabilized by n-doped carbon nanofibers for efficient hydrogen production from formic acid, *ACS Catal.* 6 (2016) 3442–3451, <http://dx.doi.org/10.1021/acscatal.6b00476>.

[52] D.S. Selishchev, P.A. Kolinko, D.V. Kozlov, Influence of adsorption on the photocatalytic properties of TiO_2/AC composite materials in the acetone and cyclohexane vapor photooxidation reactions, *J. Photochem. Photobiol. A Chem.* 229 (2012) 11–19, <http://dx.doi.org/10.1016/j.jphotochem.2011.12.006>.

[53] D. Kozlov, A. Besov, Method of spectral subtraction of gas-phase fourier transform infrared (FT-IR) spectra by minimizing the spectrum length, *Appl. Spectrosc.* 65 (2011) 918–923, <http://dx.doi.org/10.1366/11-06281>.

[54] S.E. Braslavsky, A.M. Braun, A.E. Cassano, A.V. Emeline, M.I. Litter, L. Palmisano, V.N. Parmon, N. Serpone, Glossary of terms used in photocatalysis and radiation catalysis (IUPAC recommendations 2011), *Pure Appl. Chem.* 83 (2011) 931–1014, <http://dx.doi.org/10.1351/PAC-REC-09-09-36>.

[55] J.M. Herrmann, H. Courbon, J. Disdier, M.N. Mozzanega, P. Pichat, Photocatalytic oxidations at room temperature in various media, *Stud. Surf. Sci. Catal.* 55 (1990) 675–682, [http://dx.doi.org/10.1016/S0167-2991\(08\)60200-1](http://dx.doi.org/10.1016/S0167-2991(08)60200-1).

[56] M.D. Hernández-Alonso, A.B. Hungría, A. Martínez-Arias, M. Fernández-García, J.M. Coronado, J.C. Conesa, J. Soria, EPR study of the photoassisted formation of radicals on CeO_2 nanoparticles employed for toluene photooxidation, *Appl. Catal. B Environ.* 50 (2004) 167–175, <http://dx.doi.org/10.1016/J.APCATB.2004.01.016>.

[57] A.K. Khudorozhkov, I.A. Chetyrin, A.V. Bukhtiyarov, I.P. Prosvirin, V.I. Bukhtiyarov, Propane oxidation Over $\text{Pd}/\text{Al}_2\text{O}_3$: kinetic and in situ XPS study, *Top. Catal.* 60 (2017) 190–197, <http://dx.doi.org/10.1007/s11244-017-0733-0>.